Progress In Electromagnetics Research M, Vol. 83, 203–211, 2019

A Low Bias Current Integral Type Optimal Control Scheme for a Hybrid Magnetic Bearing

Subhankar Pusti[1], Tapan Santra[2, *], and Debabrata Roy[1]

Abstract—This paper presents an application of integral type optimal control scheme for rotor positioning of a hybrid magnetic bearing (HMB) in one degree of freedom (1-DOF) using low bias current. It is observed that higher biasing current enhances the linearity and disturbance rejection capability but at a cost of higher copper loss in the actuator. So, selection of biasing in an HMB system is very crucial. In the proposed scheme the dc biasing current can be varied by adjusting the axial offset to the rotor magnet. Analysis has been conducted to achieve the optimal biasing current for better performance of the HMB. A prototype of the HMB system has been fabricated and tested which represents quite satisfactory axial vibration characteristics under low biasing current.

1. INTRODUCTION

Magnetic bearing is beneficial due to its contact free operation, zero lubrication, no wear, etc. [1]. Among the different configurations of magnetic bearing, single axis controlled hybrid bearing [2] is in the limelight recently due to its low cost and efficient performances. It integrates the benefits of active and passive [3] bearings. The peripheral devices are reduced, and the linear stiffness characteristic of the passive magnets make it efficient and cost effective. Permanent magnets abolish the requirement of control in radial direction. Axial control has been comprehended by regulating the current to the electromagnet, rightly mounted on the stator and coupling magnetically with the machine flywheel arrangement. Different control schemes: Sliding Mode Control (SMC) [4], Proportional-Integral-Derivative (PID) control [5], and H_∞ control [6] have been discussed where performances of the bearing are satisfactory but subjected to huge loss due to high biasing current. It is observed that due to the high axial stiffness of passive magnets these control schemes will not be profitable as they require high control force, leading towards saturation of the actuator.

The present work focuses on the optimal control system design of the HMB in a vertical shaft configuration. In this paper, an integral type optimal controller is proposed with variable biasing mode for the HMB system in 1-DOF. The controller gain parameters are selected to optimize the control force with efficient tracking of the reference input. The biasing current is varied to observe its impact on system response and power loss in the electromagnet coil. The controller has been designed and simulated using MATLAB to investigate the tracking performance and disturbance rejection. A prototype has been fabricated and tested in the laboratory with optimal biasing current to study the vibration characteristics, which is observed to be satisfactory in nature.

Received 19 June 2019, Accepted 1 August 2019, Scheduled 15 August 2019

* Corresponding author: Tapan Santra (tapan_santra98@yahoo.co.in).

[1] Department of Electrical Engineering, Indian Institute of Engineering Science and Technology, Shibpur, Howrah, WB 711103, India.

[2] Department of Electrical Engineering, Kalyani Government Engineering College, Kalyani, Nadia, WB 741235, India.

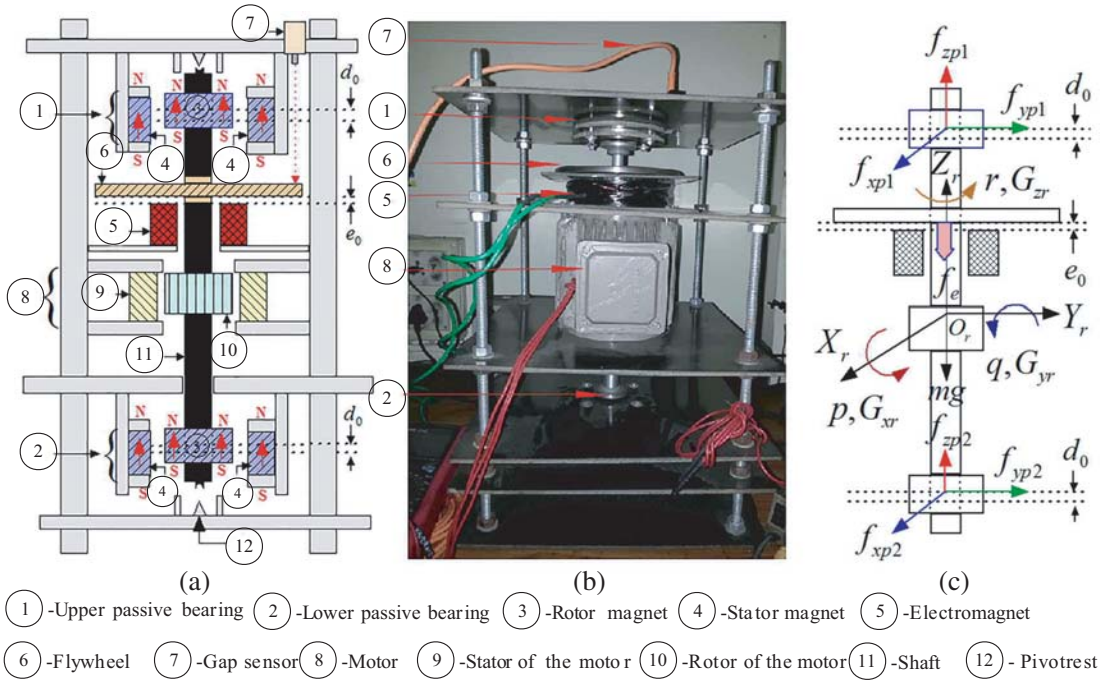

Figure 1. (a) Schematic of the Hybrid Magnetic Bearing (HMB). (b) The Laboratory prototype of the HMB. (c) Components of different forces and moments acting on the rotor in a HMB about three axes.

2. CONSTRUCTION AND WORKING PRINCIPLE OF HMB

A magnetic bearing is designed to levitate the rotor and maintain the rotor position against disturbances. Figure 1(a) shows the schematic of the proposed vertical shaft hybrid magnetic bearing. There are two passive magnetic bearings at the upper and lower portions of the machine shaft. These passive bearings consist of two concentric cylindrical type axially polarized NdFeB permanent magnets [7, 8]. The outer magnet is called stator magnet and the inner magnet called rotor magnet. The radial component of repulsive force between stator and rotor magnets inherently stabilizes the rotor in radial direction whereas axial component destabilizes the rotor in axial direction. So, to obtain axial stability, coil current is regulated in an electromagnet-flywheel arrangement as shown in Figure 1. The attractive force between the electromagnet and flywheel makes the rotor axially stable. The electromagnet has a hollow cylindrical core to accommodate the rotor shaft. A gap sensor is used to sense the axial displacement and give the feedback signal to the controller to control the coil current as per the control algorithm. Figure 1(b) shows the fabricated model of the HMB system in the laboratory.

3. MODELLING OF THE HMB

The modelling of the HMB has been represented by the authors in [4] for Six-Degree-of Freedom (6-DOF). In the present work, modelling in axial direction (1-DOF) is only considered because the HMB is passively stable in radial direction. Different forces and moments with their components about the three Cartesian axes (X, Y and Z) on the rotor are represented by Figure 1(c). The rotor magnet experiences a repulsive force due to stator magnet as shown in Figure 2. The components of these repulsive forces are f_{xp1}, f_{yp1}, and f_{zp1} at upper passive bearing and f_{xp2}, f_{yp2}, and f_{zp2} at lower passive bearing. An attractive force f_e acts between flywheel and electromagnet in axial direction. It is observed that the HMB is passively stable in radial direction by the permanent magnets but unstable in axial direction. Therefore, the axial position control is achieved by regulating the current through the coil of the electromagnet-flywheel arrangement. Furthermore, the radial and axial dynamics are decoupled in nature. So the dynamics in axial direction are of interest in this paper. The mechanical

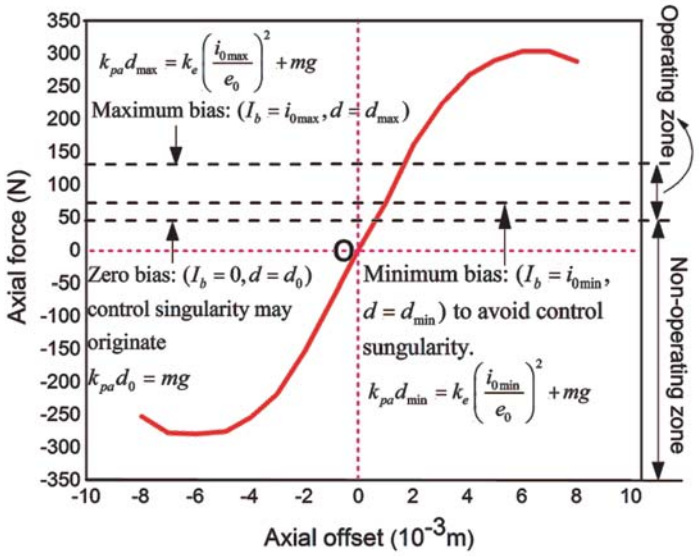

Figure 2. Variable biasing scheme for the HMB system.

and electrical dynamics in axial direction are given by Eqs. (1) and (2), respectively.

$$m\ddot{z} = (f_{zp1} + f_{zp2}) - f_e - mg + F_d \tag{1a}$$

$$\ddot{z} = \frac{2k_{pa}}{m}(z + d_0) - \frac{k_e}{m}\left(\frac{i + i_0}{z + e_0}\right)^2 - g + \frac{F_d}{m} \tag{1b}$$

$$L_e\dot{i} + R_e i = V_s \tag{2a}$$

$$\dot{i} = -\frac{R_e}{L_e}i + \frac{1}{L_e}V_s \tag{2b}$$

where z is the axial displacement, i the coil current, i_0 is the biasing current, e_0 the gap between electromagnet and flywheel, d_0 the axial offset of rotor at steady operating condition, F_d the disturbance, V_s the coil voltage, m the mass of the rotor, k_{pa} the axial stiffness of the passive magnets, k_e the electromagnet stiffness, g the gravitational acceleration, and R_e and L_e are the resistance and inductance of the electromagnet coil respectively. The axial dynamics given in Eqs. (1a)–(2b) are highly nonlinear in nature. To perform the linearization about the steady operating point, the state variables are defined as $x_1 = \triangle z$, $x_2 = \triangle \dot{z}$, and $x_3 = \triangle i$, where $\triangle$ represents the changes in the corresponding variables ($z, \dot{z}$ and i) about the steady operating point. The control force is the voltage supplied to the electromagnet coil ($U = V_s$). After linearization, the linear axial model of the HMB is given by Eqs. (3) and (4), respectively.

$$\begin{bmatrix}\dot{x}_1\\ \dot{x}_2\\ \dot{x}_3\end{bmatrix} = \begin{bmatrix} 0 & 1 & 0\\ \left(\frac{2k_{pa}}{m} + \frac{2K_e i_0^2}{me_0^3}\right) & 0 & -\frac{2k_e i_0}{me_0^2}\\ 0 & 0 & -\frac{R_e}{L_e}\end{bmatrix}\begin{bmatrix}x_1\\ x_2\\ x_3\end{bmatrix} + \begin{bmatrix}0\\ 0\\ \frac{1}{L_e}\end{bmatrix}U + F_d \tag{3}$$

$$y = \begin{bmatrix}1 & 0 & 0\end{bmatrix}\begin{bmatrix}x_1\\ x_2\\ x_3\end{bmatrix} \tag{4}$$

4. LOW BIAS CURRENT CONTROL

Biasing current is required mainly to cancel out the static load on the rotor. Although it enhances the system linearity, it increases the power loss in the HMB which may cause coil overheating, influencing

the bearing efficiency. On the other hand, reducing the bias current minimizes the power loss, but it increases the system nonlinearities and may lead to a control singularity (unbounded control voltage input). It is observed that the control current which typically depends on the dynamic load and external disturbances usually is very low. The coil current is mainly composed of biasing current. In this work, a variable biasing scheme is proposed to have a tradeoff between system response and power loss. The objective of the variable biasing scheme is to minimize the i^2R loss in the electromagnet coil after satisfying the control action. Figure 2 shows the variation of axial force between stator and rotor magnets with axial displacement. The positive stiffness signifies that for a positive (upward) axial displacement (offset) of rotor magnet, an upward magnetic force is generated which can cancel out the weight of the rotor. Bias current can be minimized by providing a suitable axial offset of the rotor as described below. Let us consider an axial offset d_0 of rotor (Figure 1(c)), which will counter-balance the weight mg of the rotor and make bias current equal to zero in the electromagnet coil as given by Equation (5).

$$k_{pa}d_0 = mg \tag{5}$$

Certainly, it decreases the total ohmic loss in the electromagnet, but it has a severe disadvantage of attracting control singularity and enhancing the system nonlinearity. This can be explained in the following ways: Let the rotor operate with a positive axial offset to cancel out the static load. When an external disturbance tries to pull down the rotor, the electromagnet current decreases as per the controller action and make the system stable. However, in this situation if the biasing current is zero at steady operating point as per Eq. (5), the system will face control singularity with unbounded control input, and the system will go out of stability. So to avoid this situation, a minimum operating current ($I_b = i_{0\,\min}$) is provided in the electromagnet coil as shown in Figure 2 and given by Eq. (6).

$$k_{pa}d_{\min} = mg + k_e\left(\frac{i_{0\,\min}}{e_0}\right)^2 \tag{6}$$

whereas the maximum bound of the biasing current is limited by the thermal capacity of electromagnet coil ($I_{thermal}$) and control current ($I_{control}$) such that Equations (7) and (8) are satisfied.

$$k_{pa}d_{\max} = mg + k_e\left(\frac{i_{0\,\max}}{e_0}\right)^2 \tag{7}$$

$$I_{0\,\max} + I_{control} \leq I_{thermal} \tag{8}$$

4.1. Design of the Controller

After considering the parameter values, given in Table 1, the state space model in Eqs. (3)–(4) of the HMB is represented by Eqs. (9) and (10), respectively.

$$\begin{bmatrix}\dot{x}_1\\ \dot{x}_2\\ \dot{x}_3\end{bmatrix} = \begin{bmatrix}0 & 1 & 0\\ 35037 & 0 & -15\\ 0 & 0 & -20\end{bmatrix}\begin{bmatrix}x_1\\ x_2\\ x_3\end{bmatrix} + \begin{bmatrix}0\\ 0\\ 2\end{bmatrix}U + F_d \tag{9}$$

$$y = \begin{bmatrix}1 & 0 & 0\end{bmatrix}\begin{bmatrix}x_1\\ x_2\\ x_3\end{bmatrix} + [0]U \tag{10}$$

Table 1. Parameters of the HMB.

Parameter	Value	Parameter	value
k_e	$6.65 \times 10^{-4}\ \frac{\mathrm{Nm}^2}{A^2}$	k_pa	$70 \times 10^3\ \frac{\mathrm{Nm}^2}{\mathrm{A}^2}$
R_e	10 ohm	L_e	0.5 H
i_0	1.9 A	d_0	0.001 m
e_0	0.005 m	m	4.5 kg

The applied voltage to the electromagnet is bounded by $\pm 100\,\mathrm{V}$. The integral control concept is used in the design. The error vector represents the difference between the reference (x_{1d}) and actual position (x_1) of the rotor system as given by Eq. (11). The corresponding augmented state vector is given by Eq. (12).

$$e(t) = x_{1d}(t) - x_1(t) \tag{11}$$

$$x_{Sigma} = \begin{bmatrix} x_1 & x_2 & x_3 & \int e dt \end{bmatrix}^T \tag{12}$$

The application of the integral control methodology gives the control law in Eq. (13), where k_1, k_2, k_3, and k_4 are the gain parameters to feedback the four state variables given by Eq. (12) respectively.

$$U = -U_{\max} \tanh\left(k_1 x_1 + k_2 x_2 + k_3 x_3 + k_4 \int e dt\right) \tag{13}$$

By minimizing the quadratic functional (14), the feedback gains can be achieved by solving Riccati equation.

$$J\left([x_\Sigma(.), U(.)]\right) = \frac{1}{2}\int_0^{t_f} \left(x_\Sigma^T Q x_\Sigma + U^T G U\right) dt \tag{14}$$

where $Q \in R^{(4\times 4)}$ is a positive-semidefinite constant-coefficient matrix, and $G \in R^{(1\times 1)}$ is the positive-definite constant-coefficient matrix, which are given by Eq. (15).

$$Q = \begin{bmatrix} 1 & 0 & 0 & 0 \\ 0 & 1 & 0 & 0 \\ 0 & 0 & 1 & 0 \\ 0 & 0 & 0 & 999995 \end{bmatrix}, \quad G = [0.01] \tag{15}$$

Now solving the Riccati Equation (16), the feedback gain matrix K is obtained.

$$-\dot{K} = Q + A_\Sigma^T + K A_\Sigma - K B_\Sigma G^{-1} B_\Sigma^T K \tag{16}$$

where the different augmented matrices are given by Eq. (17).

$$A_\Sigma = \begin{bmatrix} A & 0 \\ -C & 0 \end{bmatrix} = \begin{bmatrix} 0 & 1 & 0 & 0 \\ 35037 & 0 & -15 & 0 \\ 0 & 0 & -20 & 0 \\ -1 & 0 & 0 & 0 \end{bmatrix}, \quad B_\Sigma = \begin{bmatrix} B \\ 0 \end{bmatrix} = \begin{bmatrix} 0 \\ 0 \\ 2 \\ 0 \end{bmatrix} \tag{17}$$

The gain matrix is given by Eq. (18), and finally the bounded control law is given by Eqs. (19a)–(19b).

$$K = [K_1 \quad K_2 \quad K_3 \quad K_4]^T = \left[-4.98 \times 10^5 \quad -2.66 \times 10^3 \quad 191 \quad 3.16 \times 10^4\right]^T \tag{18}$$

$$U = -sat_{-100}^{+100}\left(-4.98 \times 10^5 x_1 + 2.66 \times 10^3 x_2 - 191 x_3 - 3.16 \times 10^4 \int e dt\right)\Big) \tag{19a}$$

$$= -sat_{-100}^{+100} f(x_1, x_2, x_3, e) \tag{19b}$$

where $f(x_1, x_2, x_3, e) = (-4.98 \times 10^5 x_1 + 2.66 \times 10^3 x_2 - 191 x_3 - 3.16 \times 10^4 \int e dt)$ and the *sat* function is given by Eqs. (20a)–(20c)

$$sat_{-100}^{+100}[f(x_1, x_2, x_3, e)] = +100 \ \ when \ \ f(x_1, x_2, x_3, e) > 100 \tag{20a}$$

$$= -100 \ \ when \ \ f(x_1, x_2, x_3, e) < -100 \tag{20b}$$

$$= f(x_1, x_2, x_3, e) \ \ otherwise \tag{20c}$$

The system is simulated using the control law in Eq. (19). The response with a step input reference is given by Figure 3(a), and corresponding control current is given in Figure 3(b). The square wave tracking and corresponding control current are represented by Figure 3(c) and Figure 3(d), respectively. It is observed that the tracking performances and disturbance rejection are excellent. A disturbance at output (Figure 3(a)) may swift away within 1 second. The control current profiles are also under desired limit and smooth.

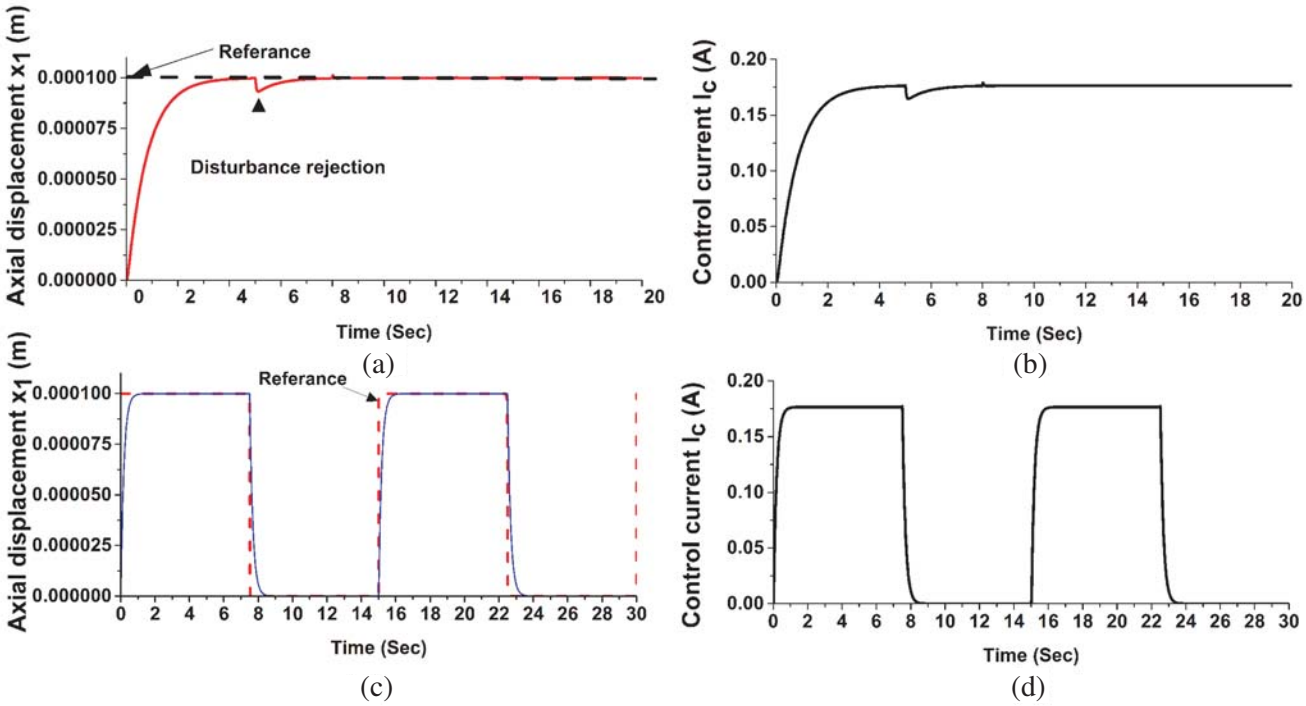

Figure 3. (a) Tracking of a step input. (b) Control current for tracking the step input. (c) Tracking a square input. (d) Control current for tracking the square input.

4.2. Effects of Biasing on Output Response

The effects of variable biasing have been investigated by changing the biasing current ($I_b = i_0$) with the same control parameters and disturbances as shown in Figure 4(a). The controller gain parameters have been selected as $k_1 = -4.04 \times 10^5$, $k_2 = -2.03 \times 10^3$, $k_3 = 203.84$, $k_4 = 3.16 \times 10^4$, and the output disturbance is considered as $x_d = 8 \times 10^{-6}$ m. It is observed that a minimum biasing ($I_b = 1.76$ A, $d_0 = 0.00091$ m) is required; otherwise, the system may become unstable (control singularity may occurs). As the biasing current increases, the linearity of the system is enhanced which makes the system more stable, but the quality of transient response degrades. It is seen that the rise time and settling time increase with biasing. So there is always a tradeoff between the stability and quality of output response if the biasing of the HMB system is changed. Another important parameter is the magnitude of external disturbance. The selection of minimum biasing partly depends on the value of the probable disturbance that may come in the system. Figure 4(b) represents the change in minimum biasing requirement with the magnitude of external disturbance. It is observed that the minimum biasing current (I_b) and axial offset of the rotor magnet (d_0) both increase with the magnitude of external disturbance. This also increases the rise time (T_r) and settling time (T_s) of the output response. The control current (I_c) decreases because of the improved linearity of the HMB system by higher biasing current. However, as the biasing current increases, the overall coil current ($I = I_b + I_c$) usually increases though the control current (I_c) is less. So it can be concluded that the increase in biasing enhances the system linearity, stability, and disturbance rejection capability, but at the same time it degrades the system responses by increasing the rise and settling times. On the other hand as the overall coil current is increased, the power loss in the HMB is also enhanced. So the biasing of the HMB should be selected very carefully.

5. PRACTICAL RESPONSES OF THE FABRICATED PROTOTYPE OF HMB

The fabricated model of the vertical shaft HMB system is shown in Figure 1(b). A photoelectric distance sensor (OADM 12U6460/S35A) is used to sense the axial displacement of the rotor. The output of the position sensor is used as the feedback signal to the controller (PIC16F877A). The controller generates

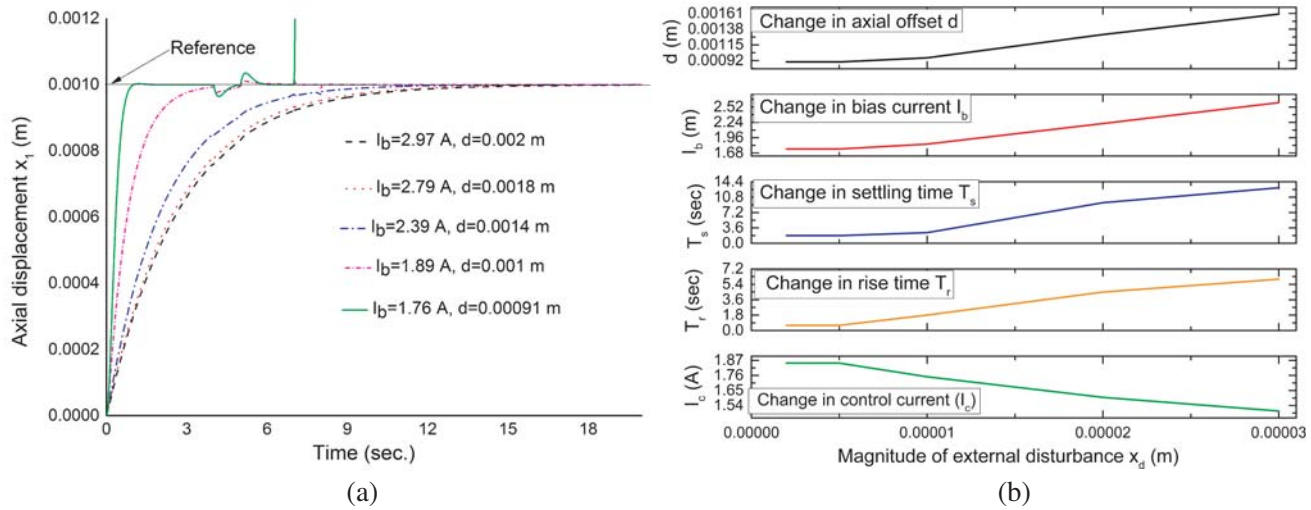

(a) (b)

Figure 4. (a) Tracking performances of HMB under varying biasing. (b) Varius control performances under varying disturbances.

the control signal to the electromagnet driver circuit to control the current in the electromagnet coil. A current sensor (LEM, LTS 25NP) is used to sense the coil current. The output of the current sensor is also given to the controller as a feedback signal. A voltage sensor is also used to measure the control voltage across the electromagnet coil. The outputs of all the sensors are displayed in a personal computer (PC) or digital storage oscilloscope (DSO) via a data acquisition system (NI, USB6009). An optimal integral type controller has been implemented. The feedback gain parameters of the controller have

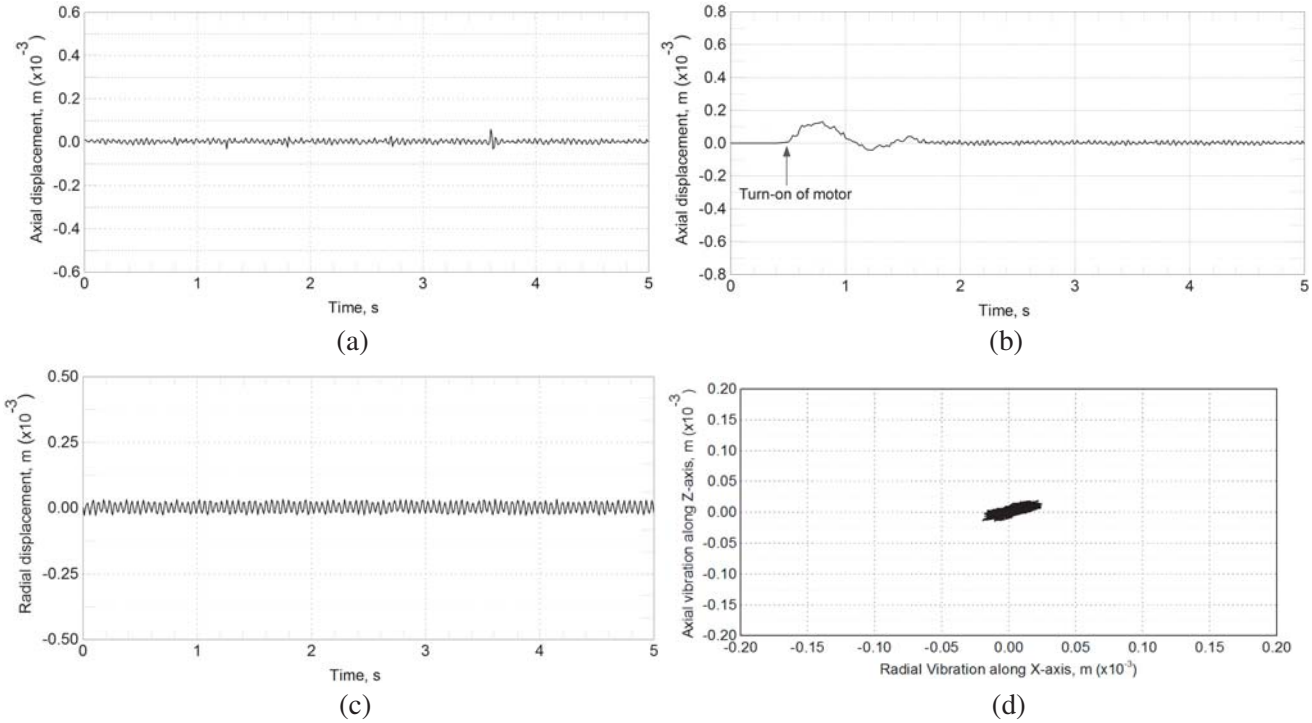

(a) (b) (c) (d)

Figure 5. (a) Axial vibration characteristic of the HMB in steady state. (b) Axial vibration at starting of the motor. (c) Radial vibration of the HMB at steady state. (d) Radial Vs Axial vibration plot.

been obtained by solving the Riccati equation using control system toolbox in MATrix LABoratory (MATLAB), as discussed in Subsection 4.1. An interactive controller program has been developed in PIC microcontroller. Using the designed controller, experiments have been carried out to stabilize the rotor. The output, axial vibration is shown in Figure 5(a). It is observed that the axial vibration is within 20 µm (peak to peak) band at steady state. A disturbance step function of 0.08 mm has been introduced by adding a suitable voltage at feedback path (with gap sensor output). The system takes approximately 0.6 sec to drive away the disturbance and come to the steady state. Figure 5(b) shows the axial vibration of the rotor due to a turn-on disturbance of the motor. At low speed of the motor, there is a huge number of harmonic torques present in the system, creating lots of disturbing forces. The motor is started and continues to run at 500 rpm. It is observed that at the time of start, the rotor undergoes a maximum axial vibration, about 0.15 mm peak. Gradually, this vibration dies out within 1.5 seconds, after which the output vibration comes to a steady state with peak to peak vibration of 18 µm. To observe the change in axial vibration with rotor speed, the rotor speed is increased to 2000 rpm. The steady state axial vibration increases to 25 µm peak to peak. So with the increase in rotor speed axial vibration slightly increases. Figure 5(c) represents the radial vibration which is under limit, and Figure 5(d) shows axial vibration (z-axis) against radial vibration (x-axis) at 1000 rpm. The radial vibration has a maximum peak of 25 µm which is sufficiently less than the air gap length of 3 mm. The axial vibration has a maximum peak of 20 µm which is quite satisfactory and under prescribed limit.

6. CONCLUSION

An integral type optimal controller has been designed to control a hybrid magnetic bearing (HMB) in one degree of freedom (1-DOF). The linear model of the HMB system is simulated to examine the tracking performance and disturbance attenuation capability of the controller. The simulated result shows the robustness of the controller with outstanding tracking of the reference as well as good disturbance ejection. The impact of the bias current on the performances of the HMB system has been observed by varying the biasing and external disturbance. It is observed that the increase in biasing enhances the system linearity, stability, and disturbance rejection capability, but at the same time it degrades the system responses by increasing the rise and settling times. Though the control current is decreased, as the biasing current increases, the overall coil current (control current + biasing current) as a whole increases, which on the other hand increases the ohmic loss in the system. So the biasing of the HMB should be selected very carefully. A prototype of the HMB system has been fabricated and tested with the proposed controller for rotor positioning in axial direction. It presents acceptable axial vibration characteristics with decent disturbance attenuation capacity. In future, zero bias current control of the HMB system can be implemented.

ACKNOWLEDGMENT

This research work is sponsored by the Science and Engineering Research Board (SERB), Department of Science and Technology, New Delhi, Government of India.

REFERENCES

1. Chen, L., et al., "Internal model control for the AMB high-speed fly wheel rotor system based on modal separation and inverse system method," *IET Electric Power Applications*, Vol. 13, No. 3, 349–358, 2019.
2. Ohji, T., Y. Katsuda, K. Amei, et al., "Structure of one-axis controlled repulsive type magnetic bearing system with surface permanent magnets installed and its levitation and rotation tests'," *IEEE Trans. on Magnetics*, Vol. 47, No. 12, 4734–4739, 2011.
3. Han, B., S. Zheng, X. Wang, and Q. Yuan, "Integral design and analysis of passive magnetic bearing and active radial magnetic bearing for agile satellite application," *IEEE Transaction on Magnetics*, Vol. 48, No. 6, 1959–1966, 2017.

4. Santra, T., D. Roy, A. B. Choudhury, and S. Yamada, "Vibration control of a hybrid magnetic bearing using an adaptive sliding mode technique," *Journal of Vibration and Control*, Vol. 24, No. 10, 1848–1860, 2018.
5. Wei, C. and D. Söffker, "Optimization strategy for PID controller design of AMB rotor system," *IEEE Transaction on Control System Technology*, Vol. 24, No. 3, 788–803, 2016.
6. Komorii, M. and N. Akinagar, "A prototype of flywheel ebergy storage system suppressed by hybrid magnetic bearing with H/sup/spl infin// controller," *IEEE Transactions on Applied Super Conductivity*, Vol. 11, No. 1, 1733–1736, 2001.
7. Santra, T., D. Roy, and A. B. Choudhury, "Calculation of passive magnetic force in a radial magnetic bearing using general division approach," *Progress In Electromagnetics Research M*, Vol. 54, No. 1, 91–102, 2017.
8. Santra, T., D. Roy, and S. Yamada, "Calculation of force between two ring magnets using adaptive monte carlo technique with experimental verification," *Progress In Electromagnetic Research M*, Vol. 49, No. 1, 181–193, 2016.